Journal of
Composites Science

MDPI

Article

Thermomechanical and Pre-Ignition Properties of Multicomponent Poly(Vnylidene Fluoride)/Aluminum Oxide/Single-Walled Carbon Nanotube Hybrid Nanocomposites

Ruchinda Gooneratne and Jude O. Iroh *

Department of Mechanical and Materials Engineering, University of Cincinnati, Cincinnati, OH 45221, USA
* Correspondence: irohj@ucmail.uc.edu

Abstract: Poly(vinylidene fluoride), PVDF is a piezoelectric semi-crystalline fluoroplastic that is widely used in the electronics and semiconductor industry for packaging, sensors, and actuators. PVDF nanocomposites containing single-walled carbon nanotubes, SWCNTs and fumed alumina, Al_2O_3 were prepared in dimethylformamide, and their thermal and dynamic mechanical properties were determined by using thermogravimetric analysis, TGA, differential scanning calorimetry, DSC and dynamic mechanical analysis, DMA. It was observed from differential scanning calorimetry that the matrix's degree of crystallinity and enthalpy of melting was reduced in the presence of the nanofillers to about 7.1%, compared to the neat PVDF whose degree of crystallinity was determined to be about 51.3%. The melting temperature, Tm obtained by DSC measurements was also reduced from 171.6 °C to 162.7 °C at high SWCNT loadings. The onset degradation temperature was also lowered in the presence of the nanofillers, especially alumina particulates. Dynamic mechanical analysis of the composites showed a significant improvement in the storage modulus of about 18 GPa in the presence of SWCNT. The glass transition temperature, T_g was significantly increased from −42.6 °C to −33.2 °C due to reinforcement with SWCNT. The reinforcement of PVDF with SWCNT and alumina resulted in greater char retention at 600 °C.

Keywords: poly(vinylidene fluoride); alumina; single-walled carbon nanotube; ternary hybrid nanocomposites; thermomechanical properties; pre-ignition temperature; thermal transition temperatures

check for updates

Citation: Gooneratne, R.; Iroh, J.O. Thermomechanical and Pre-Ignition Properties of Multicomponent Poly(Vnylidene Fluoride)/Aluminum Oxide/Single-Walled Carbon Nanotube Hybrid Nanocomposites. *J. Compos. Sci.* **2022**, *6*, 380. https://doi.org/10.3390/jcs6120380

Academic Editor: Francesco Tornabene

Received: 15 October 2022
Accepted: 30 November 2022
Published: 12 December 2022

Publisher's Note: MDPI stays neutral with regard to jurisdictional claims in published maps and institutional affiliations.

Copyright: © 2022 by the authors. Licensee MDPI, Basel, Switzerland. This article is an open access article distributed under the terms and conditions of the Creative Commons Attribution (CC BY) license (https://creativecommons.org/licenses/by/4.0/).

1. Introduction

Poly(vinylidene fluoride) (PVDF) is a smart semicrystalline fluoropolymer produced by the polymerization of vinylidene fluoride. It has many applications in a wide range of fields due to its ease of processing, chemical resistance, excellent mechanical properties, and low thermal conductivity [1–3]. It is also known to possess piezoelectric properties and is widely used in the electronic, biomedical, and construction industries, as sensors and actuators [2,4,5]. PVDF crystallizes into five different polymorph phases: α, β, δ, ϒ, and ε with each phase having useful properties and α being the most common [1,6]. The piezoelectric prominent β phase according to Kabir et al. [6], can be stabilized by the introduction of nanofillers. This phase has been reported to have the highest melting point by Feng [7]. The fluoropolymer is soluble in a range of solvents and also acts as a very powerful binding matrix for a wide range of nanofillers, enabling it to share and enhance their properties [8,9]. Some studies have also looked at PVDF sponge-like membrane material for many applications ranging from water/oil separators to antibacterial sponges [10]. The reinforcement of PVDF by nanofillers has been performed to improve certain properties such as the thermal and mechanical properties of PVDF which is known to have melting temperatures ranging from 164 °C [7] to 173 °C. The melting temperature

of PVDF nanocomposites containing barium titanate, $BaTiO_3$ and reduced graphene oxide varies from 164 °C [7] to 173 °C according to Mokhtari's group [11].

Single-walled carbon nanotubes (SWCNTs) have become very useful nanofillers for polymer matrices due to their low densities, high electrical and thermal conductivities, high aspect ratios, and excellent tensile strength. Overall polymer-SWCNT nanocomposites have high thermo-mechanical properties [1,12]. Ma et al. studied the effect of dispersing functionalized SWCNTs in a PVDF matrix, and they reported an improved degree of crystallinity of about 55.6% compared to 53.1% for the neat PVDF at low CNT loadings. Ghosh's team was able to utilize the highly electrically and thermally conductive nature of CNTs to make composites with effective EMI shielding ability [13]. However, the thermal stability obtained by monitoring the thermal decomposition of the composites was lowered from 459 °C to 430 °C at low loading due to the creation of defects on the CNT surface [1]. In another related study by Du, it was observed that a slight increase in the melting point upon the addition of multi-walled carbon nanotubes, MWCNTs from 163 °C to 166.5 °C [14] occurred. MWCNTs were also shown to directly improve the storage moduli of the PVDF composites by Pereira [15]. According to Chiu, the storage modulus of the PVDF nanocomposite was improved by about 1.53 GPa at 25 °C in a similar system containing graphene nanoparticles [16].

Fumed alumina (Al_2O_3) is another interesting nanofiller that has been studied as a solid fuel propellant and energetic material [17–19]. McCollum's group studied alumina-PVDF composites and did not find any improvement in the melting temperature (T_m) and decomposition temperature (T_d). A lower T_d was obtained due to the addition of alumina to PVDF from 459 °C to 395 °C. However, the degree of crystallinity was significantly improved [19]. The objective of this work is to study the effect of introducing both SWCNTs and Alumina nanofillers on the thermal and mechanical properties of the hybrid PVDF-based nanocomposites. Furthermore, the effect of alumina on the pre-ignition behavior of PVDF is also investigated.

2. Materials and Methods

2.1. Materials

The materials used for this study include reagent-grade (ACS) N,N-Dimethylformamide (DMF) purchased from Right Price Chemicals, and Aluminum oxide (highly dispersed-fumed), provided by Evonik Industries (Essen, Germany) in the form of AEROXIDE® Alu C. Poly(vinylidene fluoride) (PVDF) was purchased from Sigma Aldrich and single-walled carbon nanotubes (SWCNTs) were obtained from Tuball™ (Luxembourg). All chemicals were used as received.

2.2. Preparation of PVDF/CNT/Al_2O_3 Composites

PVDF powder was dispersed in 50mL of DMF under mechanical stirring at about 550 rpm for 2 h at room temperature. A colorless polymer solution was obtained. Aluminum oxide of a predetermined mass was later dispersed into this PVDF solution under both mechanical stirring and probe ultrasonication (pulsed) for 2 h.

SWCNTs were dispersed by mechanical stirring and ultrasonication for 2 h in 50 mL DMF. The uniform SWCNT dispersion was then transferred into the PVDF or PVDF/Aluminum oxide solution and then homogenized by following the above procedure for 4 h, forming a homogenous viscous slurry. All dispersions were prepared at 5 °C in a water bath equipped with a condenser to produce the following samples containing the below-stated wt.% of fillers (Table 1).

Table 1. Composition of the nanocomposites.

Composite	PVDF (wt.%)	SWCNT (wt.%)
Neat PVDF	100	0
CNT 5 PVDF	95	5
CNT10 PVDF	90	10
CNT 50 PVDF	50	50
Al_2O_3 1 PVDF	99	0
Al_2O_3 5 PVDF	95	0
Al_2O_3 10 PVDF	90	0
Al_2O_3 50 PVDF	50	0
CNT 1 Al_2O_3 1 PVDF	98	1
CNT 5 Al_2O_3 1 PVDF	94	5
CNT 1 Al_2O_3 5 PVDF	94	1
CNT 10 Al_2O_3 1 PVDF	89	10
CNT 1 Al_2O_3 10 PVDF	89	1
CNT 5 Al_2O_3 5 PVDF	90	5
CNT 10 Al_2O_3 10 PVDF	80	10

Thin films of each sample were prepared using an MTI vacuum-assisted film coater (coated at 0.5 mm wet thickness) over a Teflon sheet. Initial curing was done at 100 °C until all visible solvent was dried out for 1 h. The samples were then transferred and post-cured in a vacuum oven at 130 °C for 2 h to remove any residual DMF, producing the final thin films for characterization.

2.3. Characterization

To understand the thermal characteristics of the nanocomposite, thermogravimetric analysis (TGA) and differential scanning calorimetry (DSC) was performed by using TA Instruments Q50 and Q20, respectively. All measurements were carried out in a nitrogen atmosphere at a ramp rate of 5 °C/min starting from room temperature. TGA measurement was run up to 600 °C and DSC was performed from room temperature to 450 °C. The polymer nanocomposite melting temperature (T_m), enthalpy of melting (ΔH_m), and degree of crystallinity (χ_c) were obtained from the above analytical techniques.

Dynamic mechanical analysis was carried out using an EXSTAR6000 DMA purchased from Seiko Instruments Inc to study the nanocomposite's thermo-mechanical response. The properties obtained from the DMA study include the storage modulus (E′), loss modulus (E″), and tan delta (δ). DMA of neat PVDF and the respective nanocomposites were carried out in the tensile mode. These tests were performed at a temperature range of −60 °C to 160 °C and a ramp rate of 10 °C/min. All measurements were carried out at an oscillatory frequency of 1 Hz.

3. Results and Discussion

3.1. Differential Scanning Calorimetry (DSC)

DSC was used to study the effect of filler type and loading on the melting behavior of the matrix. The area under the melting peaks was observed and used to determine the degree of crystallinity (χ_c) using a 100% crystalline PVDF heat of fusion (ΔH_o) of 105 J/g as reference according to the formula [1]:

$$\chi_{c=\frac{\Delta H_m}{\Delta H_o}\times 100\%} \quad (1)$$

The enthalpy of melting (ΔH_m) was obtained by the integrated area of these melting peaks. Results of these calculations are summarized in Table 2 with their DSC traces shown in Figures 1–4. Neat PVDF shows a sharp endothermic peak at 171.6 °C, indicating its melting point as confirmed by many other similar studies [1,11,20]. A degree of crystallinity of about 51% was calculated for PVDF using Equation (1). Figures 1 and 2b also shows the occurrence of pre-ignition exotherm for Al_2O_3/PVDF nanocomposites between 200 °C

and 250 °C. The pre-ignition temperature seems to decrease with increasing alumina loading. The DSC thermograms also show the decomposition behavior of the alumina/PVDF nanocomposites. At low alumina wt.% of 1 and 5 wt.%, a doublet decomposition endothermic peak, located between 275 °C and 300 °C with a slight shoulder at 375 °C was observed.

Table 2. shows the melting temperature (T_m), enthalpy of melting (ΔH_m), and degree of crystallization (χ_c) for each nanocomposite.

Composite	T_m (°C)	ΔH_m (J/g)	χ_c (%)
Neat PVDF	171.6	53.2	50.67
CNT 5 PVDF	168.9	56.4	53.71
CNT10 PVDF	168.6	54.7	52.10
CNT 50 PVDF	162.7	7.4	7.05
Al_2O_3 1 PVDF	170.2	57.0	54.29
Al_2O_3 5 PVDF	170.0	38.0	36.19
Al_2O_3 10 PVDF	170.8	52.1	49.62
Al_2O_3 50 PVDF	171.0	21.5	20.48
CNT 1 Al_2O_3 1 PVDF	172.6	64.6	61.52
CNT 5 Al_2O_3 1 PVDF	169.7	47.2	44.95

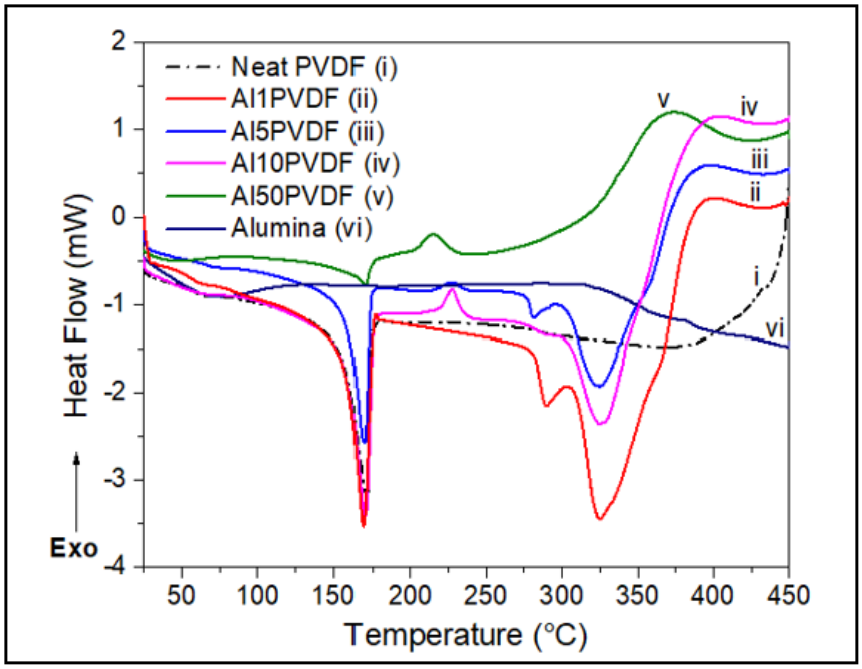

Figure 1. DSC comparisons of effect of Alumina wt.% loadings on PVDF thermal properties.

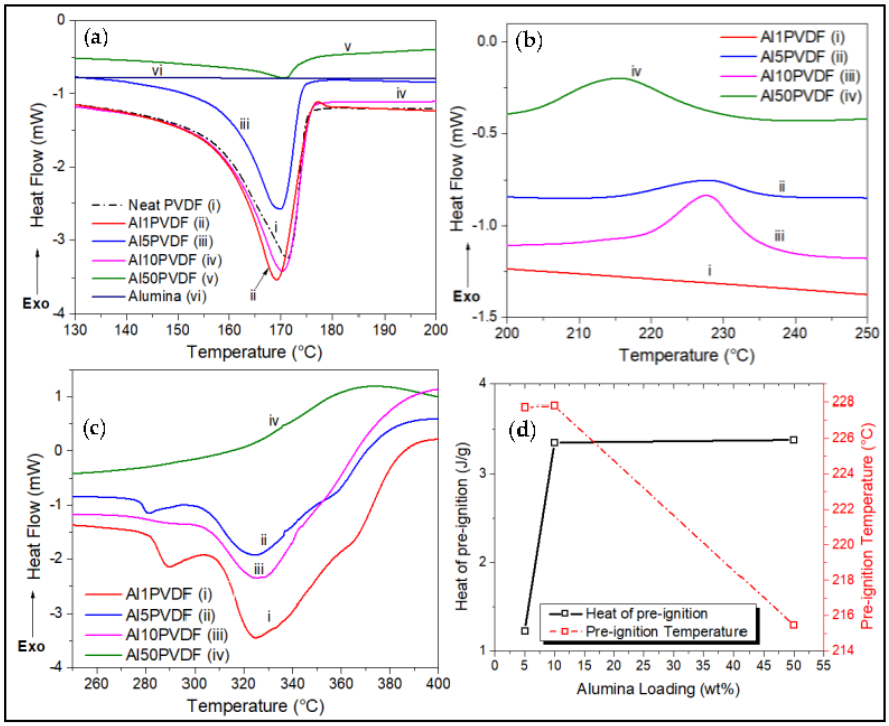

Figure 2. DSC thermograms of varying Alumina wt.% loadings on PVDF, showing (**a**) endothermic melting peaks, and pre-ignition exotherms between (**b**) 200 °C and 250 °C and between (**c**) 250 °C and 400 °C, carried out under N_2 atmosphere. (**d**) Degree of crystallization and melt peak temperature trend with loading.

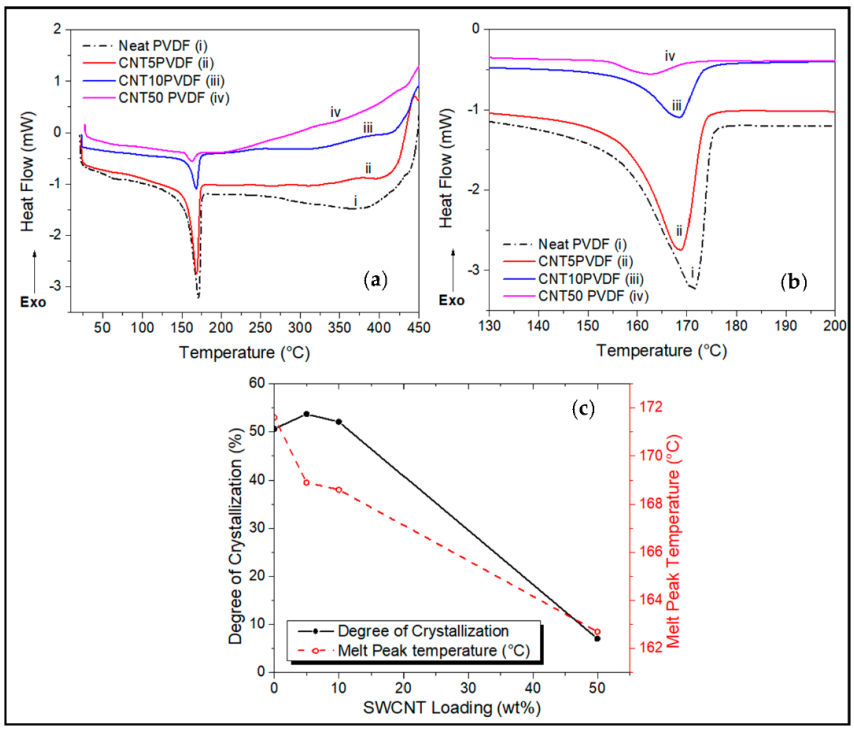

Figure 3. DSC comparisons of (**a**) CNT wt.% loadings on PVDF, showing (**b**) endothermic melting peaks carried out under N_2 atmosphere. (**c**) Degree of crystallization and melt peak temperature trend with loading.

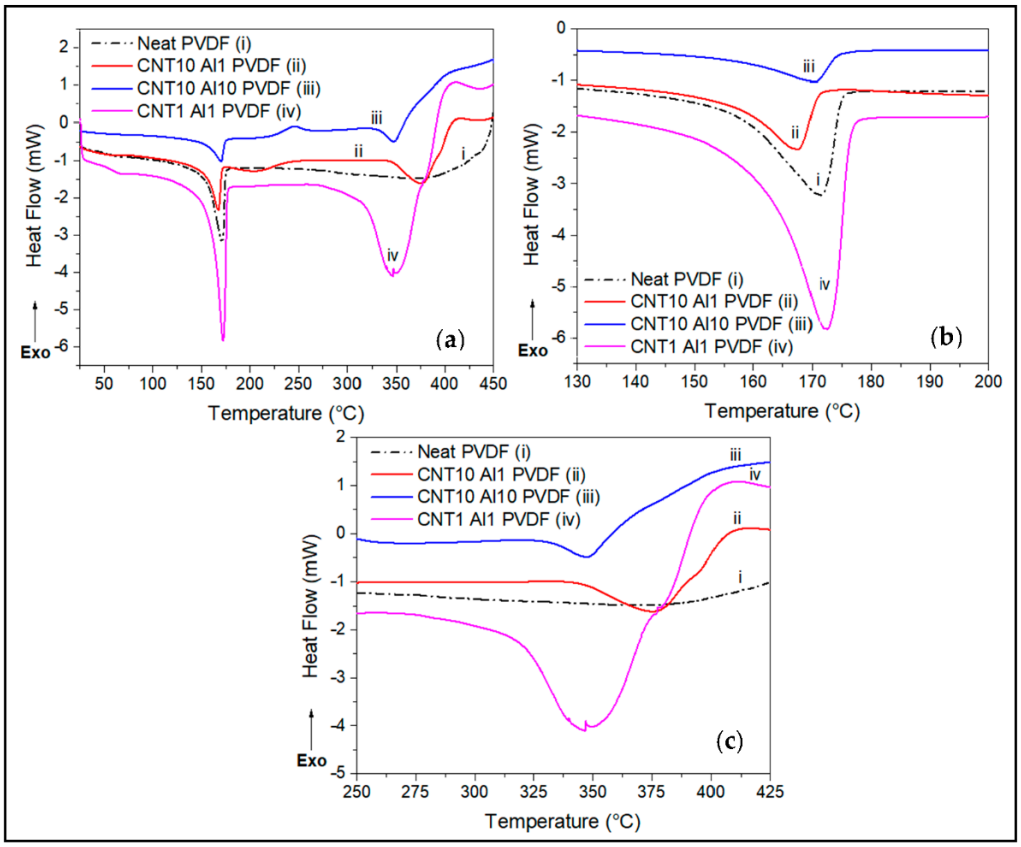

Figure 4. DSC **thermograms** comparisons of (**a**) **effect of** combinatorial CNT/Alumina wt.% loadings on PVDF, showing (**b**) endothermic melting peaks between 130 °C and 200 °C, and (**c**) peaks between 250 °C and 425 °C.

The dispersion of fumed alumina in the PVDF to form alumina/PVDF nanocomposite results in a slight reduction in the melting point (T_m) compared to the neat PVDF. There appears to be a direct relationship between the alumina loading and the T_m of the nanocomposite. The T_m was raised from 170.2 °C to about 171.0 °C when the loading of Al_2O_3 is increased from 1 to 50 wt.%. However, this has an inverse effect on the material's degree of crystallinity, dropping it from 54% to 20%. Figure 2 shows the expanded DSC thermograms for alumina-PVDF samples.

An interesting trend in the behavior of alumina/PVDF nanocomposite is shown in the DSC traces in Figure 2a concerning the CNT/PVDF and neat PVDF in Figure 3. Small exothermic peaks located between 215 °C and 230 °C, are observed at 5, 10, and 50 wt.% alumina in PVDF (Figure 2b) as well as for 10 wt.% alumina in the ternary Al10/CNT10/PVDF composite at around 245 °C (Figure 4a). This phenomenon is due to preignition occurring between the alumina and PVDF [17,20,21]. Research into this has suggested that the melting of PVDF is accelerated by the presence of alumina nanoparticles reacting with the fluoride radical to form aluminum fluoride, AlF_3. This fluorination reaction that forms AlF_3 reduces the degradation temperature of the nanocomposite at higher loadings of alumina into the PVDF matrix [22,23].

The effect of reinforcing PVDF with SWCNTs is the lowering of the enthalpy of melting as can be seen by the depression in the endothermic melt peak (Figure 3a–c), resulting in a significant decrease in the degree of crystallization to as low as 7% at CNT loadings of 50 wt.%. The addition of CNT fillers into PVDF also significantly reduces the melting temperature as well as the degree of crystallization to as low as 162 °C and 20%, respectively, compared to the neat PVDF system as seen in Figure 2c,d.

The drop in melting temperature can be attributed to changes in the semicrystalline structure of the PVDF matrix. According to a study by Xiao's group [24], it is reported that as the crystallinity of a polymer decreases, so does its thermal conductivity. This change in morphology could be attributed to a decrease in the polymer matrix's lamella thickness as the wt.% of SWCNT in the system is increased [8,24]. At lower wt.% (<50 wt.%) loadings of SWCNT a slightly higher degree of crystallization is obtained because they are known to be effective nucleating agents in semicrystalline polymer matrices [7,16]. This could be due to better and more efficient dispersibility and localization of the SWCNTs in the matrix [15,24]. However, at higher wt.% this effect is reversed as the rigid nanofiller network impedes polymer chain movement, reducing the crystalline nature of the matrix [14,24,25].

Figure 4 shows the effect of hybrid Al_2O_3 and SWCNT fillers on the melting and decomposition behavior of PVDF. The hybrid nanofillers lower the degree of crystallinity and decomposition temperature of the matrix (Figure 4b,c). The hybrid Al_2O_3 reinforcement of PVDF, accordingly, produced a relatively lower melting peak area than that for the neat PVDF matrix. When one compares the effect of SWCNT and alumina on the matrix, it is shown that SWCNTs of the same wt.% led to a greater drop in the degree of crystallinity because it forms a much denser percolated network [24]. However, the synergistic and catalytic effect of the two fillers is shown at lower loading of 1 wt.%, for which the highest degree of crystallization and enthalpy of melting were recorded, compared to the individual nanofillers and the neat matrix.

3.2. Thermogravimetric Analysis (TGA)

TGA analysis was used to study the thermal stability of each nanocomposite and the effect each nanofiller has on its performance in a N_2 atmosphere. TGA and their respective derivative traces of the samples are plotted in Figures 5–7. The thermal stability measured from 5% weight loss is about 435 °C for neat PVDF but decreases with increasing filler loading (Figures 5a, 6a and 7a). The onset temperature of degradation of PVDF occurs at about 420 °C and the temperature for the maximum rate of decomposition with the greatest rate of weight loss occurs at 451 °C (Figure 5a,b).

At 600 °C, PVDF has nearly completely degraded, retaining only about 37% of its original mass. This drastic drop in the weight of PVDF is due to hydrogen fluoride gas produced by the decomposition of PVDF [3,20]. Char retention of alumina/PVDF composite increases with increasing alumina loading, reaching a value of 46% at 50 wt.% loading.

The addition of both nanofillers, individually and in combination shows a decrease in the thermal stability of the nanocomposite relative to the neat PVDF matrix. Alumina reduces the temperature for the onset of degradation to around 290 °C at 1 wt.% and 220 °C at 50 wt.% loading as shown in Figure 5a. Higher alumina content (50 wt.%) yielded the highest residual mass of around 46% at 600 °C. The highest rate of weight loss for these alumina/PVDF composites occurred between 320 °C and 340 °C (Figure 5b). Figure 5c shows that the DTG peak area for decomposition of the nanocomposites decreases with increasing alumina content, suggesting decreasing nanocomposite decomposition rate with increasing wt.% of alumina.

This early degradation of alumina-reinforced PVDF nanocomposites is due to the preignition phase occurring between fluoride radical and alumina showed after the melting of PVDF in the presence of alumina, as shown in the previous section. Alumina serves as a catalyst by forming active sites.

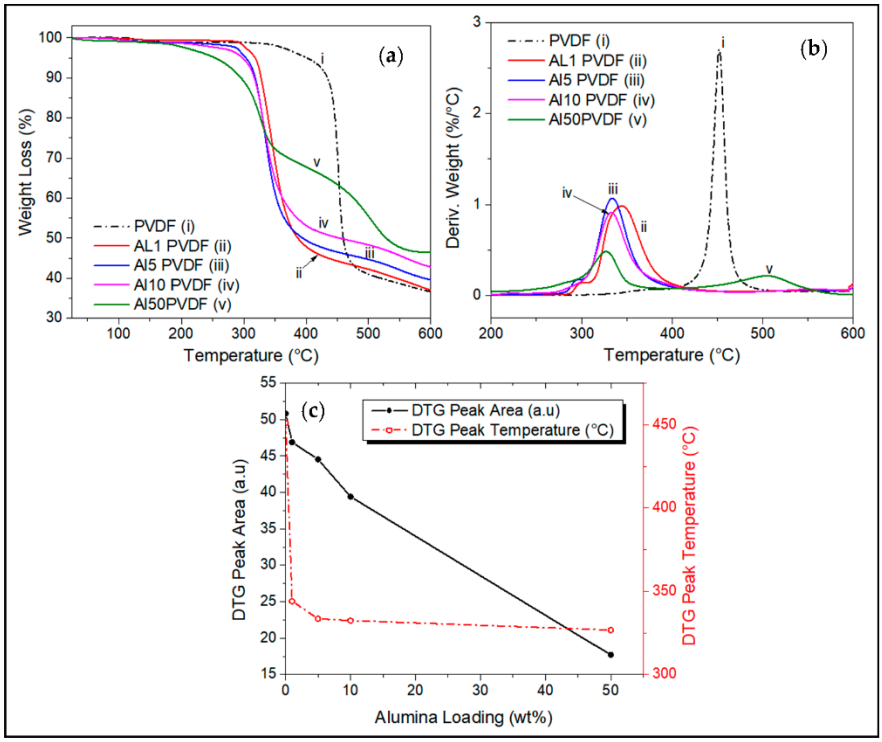

Figure 5. (**a**) TGA thermogram comparisons of effect of Alumina loading on PVDF, with their respective (**b**) derivative weight curves, carried out from room temperature to 600 °C under N_2 atmosphere. (**c**) effect of alumina loading on the DTG peak area and peak temperature.

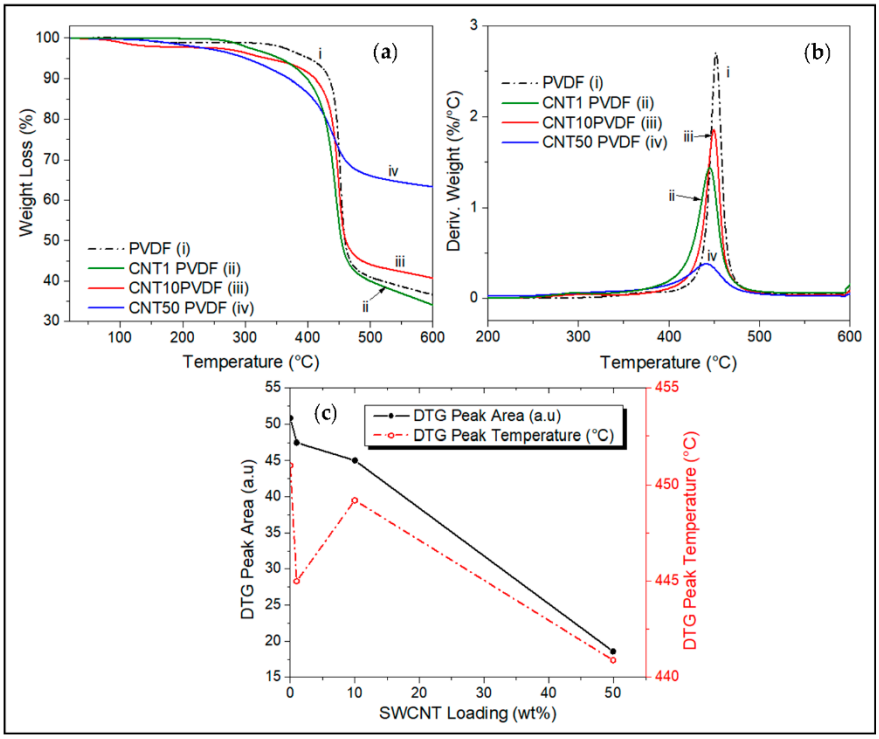

Figure 6. (**a**) TGA thermogram comparisons of the effect of CNT wt.% loadings on decomposition of PVDF, with their respective (**b**) derivative weight curves, TGA test was carried out from room temperature to 600 °C under N_2 atmosphere. (**c**) effect of CNT loading on the DTG peak area and peak temperature.

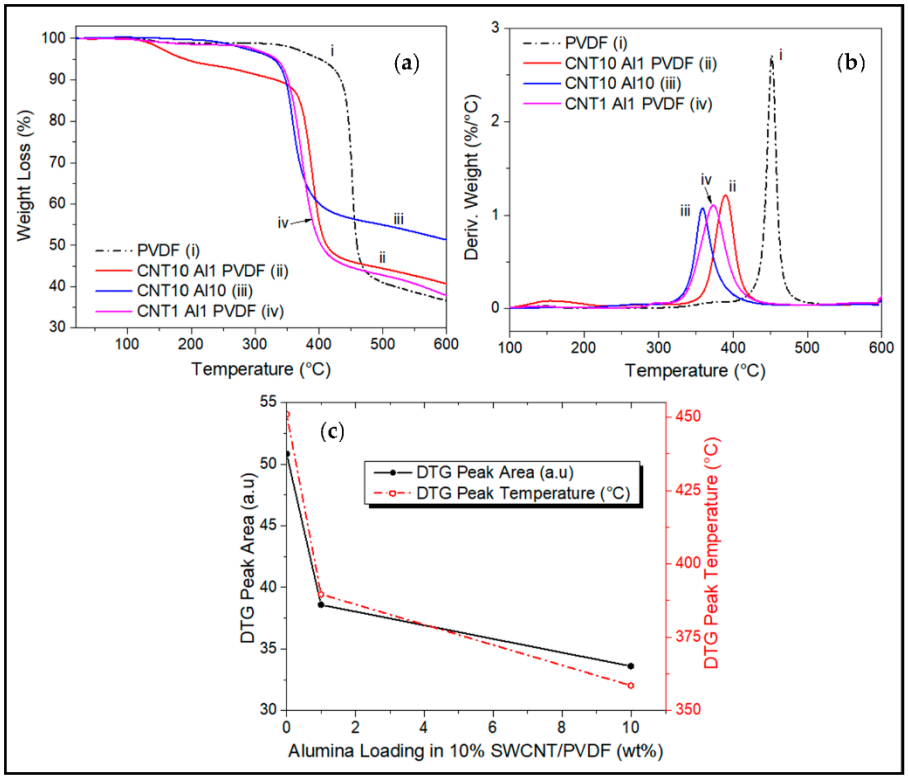

Figure 7. (**a**) TGA thermogram comparisons of **effect of** combinatorial CNT and Alumina wt.% loadings on **decomposition of** PVDF, with **the** respective (**b**) derivative weight curves. **TGA test was** carried out from room temperature to 600 °C under N_2 atmosphere. (**c**) **effect of composition on** DTG peak area and **peak** temperature.

Figure 6a–c show the effect of SWCNT loading on the decomposition behavior of SWCNT/PVDF nanocomposites. Increasing the wt.% of SWCNT in the nanocomposites decreases the thermal stability **and increases the char retention** of the composite (Figure 6a,b), decreases the DTG peak height at a maximum rate of decomposition, and decreases the decomposition rate (Figure 6b,c). At SWCNT loading > 1 wt.%, increasing the weight fraction of SWCNT results in increasing char yield and char retention over 60%, obtained at 50 wt.% of the nanofiller (Figure 6a). A similar pattern is seen in the variation of SWCNT composition in Figure 6, but less pronounced than the effect produced by alumina/PVDF (Figure 5). A shift to a slightly lower temperature for the onset of degradation is observed around 400 °C as SWCNT loading is increased. However, the temperature at which the highest rate of weight loss occurs remains almost the same at around 450 °C, and the rate of degradation decreases with increasing SWCNT weight fraction (Figure 6b). A high residual mass of 63% is observed at 600 °C for a sample containing 50 wt.% CNT.

Figure 7 shows the effect of hybrid Al_2O_3/SWCNT fillers on the thermal stability of the nanocomposites. Reinforcement of PVDF with the hybrid fillers lowers the thermal stability of the matrix (Figure 7a,b) but lowers the decomposition rate (Figure 7b,c). It was reported that the thermal decomposition of PVDF at lower temperatures, produces hydrogen fluoride [18,19,26]. The fluorination reaction speeds up and causes the matrix to decompose at a lower temperature, leading to its early onset of degradation [17,23].

The preignition phenomenon, reported earlier, caused by alumina is also shown in the ternary Al_2O_3/SWCNT/PVDF system in Figure 7a. At higher alumina loading in the hybrid nanocomposite, for instance, Al10/CNT10/PVDF composite containing 10 wt.% alumina, results in a lower onset of degradation temperature of 330 °C and a high char yield of 51% at 600 °C compared to Al1/CNT10/PVDF with 1 wt.% of alumina which has a decomposition temperature of 360 °C and char yield of about 40%.

This decrease in thermal stability for a nanocomposite containing carbon nanotubes is unusual, given its incredible thermal characteristics and ability to create a thermally conductive network, and form a char barrier, protecting the matrix [12,16,27]. However, some studies have also identified occasions where CNT has the opposite effect. According to Pereira's work [15], it was identified that the CNTs introduced a higher shear stress concentration factor during the polymer blending process which in turn disrupts the structure of the polymer chain. Yang also reported similar observations of a decrease in the thermal stability of acrylonitrile-butadiene-styrene (ABS) in the presence of CNT. It is believed that CNT is involved in the formation of radicals which catalyzes the degradation process of ABS which in turn is degraded by hydrogen abstraction, hydroperoxide formation, and unzipping processes [28]. The radical formation mechanism could also be the likely cause of the reduced thermal stability of the CNT/PVDF nanocomposite resulting from the thermal degradation of PVDF [3,29]. Table 3 summarizes the temperature for 5% weight loss and char yield (%) obtained at 600 °C.

Table 3. Summary of TGA results showing 5% weight loss temperature and char yield at 600 °C.

Composite	5% Weight Loss Temp. (°C)	Char Yield at 600 °C (%)
Neat PVDF	401.5	36.5
CNT1 PVDF	354.6	34.0
CNT10 PVDF	334.2	40.7
CNT 50 PVDF	300.7	63.3
Al1PVDF	318.0	36.9
Al5PVDF	303.2	39.5
Al10PVDF	297.8	42.7
Al50PVDF	253.7	46.4
CNT 1 Al_2O_3 1 PVDF	333.0	37.8
CNT 10 Al_2O_3 1 PVDF	190.4	40.6
CNT 10 Al_2O_3 10 PVDF	328.6	51.3

3.3. Dynamic Mechanical Analysis (DMA)

DMA study provides useful insight into the viscoelastic nature of the nanocomposite variants. Figure 8a shows the variation of storage modulus with temperature and composition for neat PVDF and its nanocomposites while Figure 8b shows the variation of tan δ peaks for α and ϒ transitions for the neat PVDF and its nanocomposites. The tan δ peak area and height are indicative of the damping ability of the material. For linear amorphous polymers, the temperature corresponding to the apex of the α-peak is the glass transition temperature (T_g). However, for semicrystalline polymers, the α-peak is associated with the melting temperature, while the ϒ-peak is associated with the glass transition relaxation. In this work, the melting temperature, (T_m) is observed at very low temperatures (Figure 8c).

The addition of 50 wt.% SWCNT into the PVDF matrix is shown to significantly increase the storage modulus to 18 GPa at −55 °C compared to neat PVDF, which has a glassy region storage modulus of about 4.24 GPa (Figure 8a). The difference in the storage moduli of the neat matrix and the reinforced nanocomposites at high loading (50 wt.%), could be due to an increase in the stiffness of the composite upon reinforcement with uniformly dispersed nanofillers in the matrix [5,11,25]. However, at 10 wt.% SWCNT loading, the composite's storage modulus was slightly lower than that of neat PVDF. All samples show a decrease in their storage moduli at higher temperatures.

At low combinatorial loading of SWCNT and alumina of 1 wt.% each, the hybrid composite was observed to have a similar storage modulus as the neat PVDF matrix of about 3.7 GPa, and the hybrid nanocomposites had higher temperature stability up to 120 °C before their storage modulus started to decrease. The Al1/PVDF composite showed the lowest thermomechanical stability, enduring only up to 55 °C before its modulus dropped sharply (Figure 9a). Figure 9b shows the variation of the tan δ peak for chain relaxation (ϒ) for the neat PVDF and alumina/PVDF nanocomposite containing 1 wt.% alumina. The T_g for the neat matrix and the nanocomposite with 1 wt.% alumina is about

−40 °C for both. The melting point for the neat PVDF matrix is shown to be about 125 °C (Figure 9c) which is significantly lower than that obtained from DSC of about 173 °C (Figure 3a,b and Figure 4a,b).

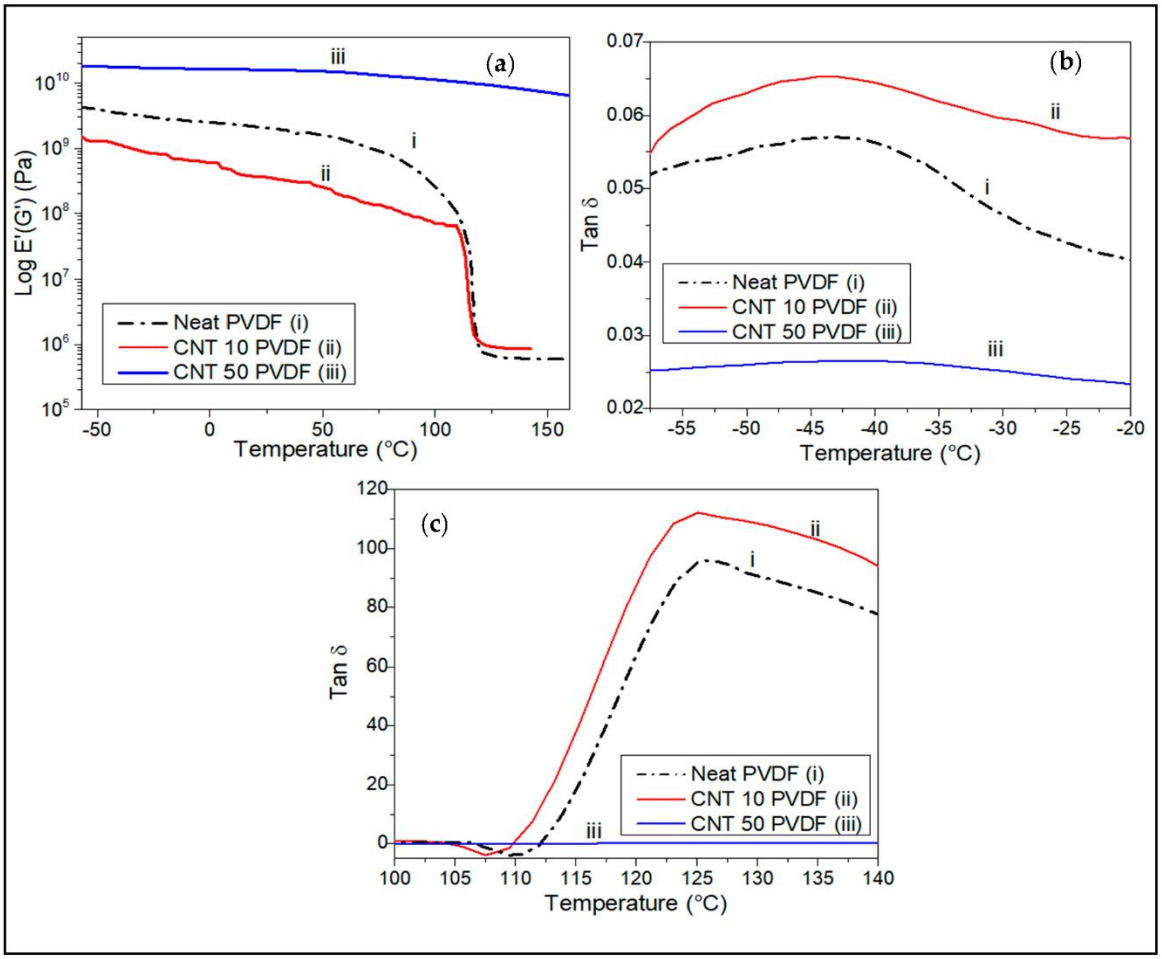

Figure 8. DMA plots comparing the (**a**) effect of CNT loading on the storage modulus of the PVDF CNT at an oscillatory frequency of 1Hz under tension. Tan delta peaks show (**b**) dynamic T_g between −55 °C and −20 °C and (**c**) T_m between 105 °C and 140 °C.

Figure 10 shows the effect of hybrid alumina-SWCNT fillers on the dynamic mechanical behavior of Al_2O_3/SWCNT/PVDF hybrid nanocomposites. In Figure 10b the Tan δ versus temperature curves for the samples at low temperatures show that the incorporation of nanofillers increased the glass transition temperature of the nanocomposite. This is because the introduction of fillers in the matrix reduces its free volume and hence restricts chain motion to a certain degree, requiring more energy in the form of heat for chain motion [11]. Neat PVDF has a T_g of −42.6 °C while the incorporation of higher alumina loading into the matrix increased the T_g to about −33.2 °C for Al10/CNT1/PVDF. A 50 wt.% loading of SWCNT in the nanocomposite did not show a prominent ϒ-relaxation peak. Table 4 summarizes the thermal transition temperatures obtained from DMA measurements. Figure 10a,c show the melting temperature of the samples at 119 °C ≤ T_m ≤ 129 °C. A much lower melting temperature for the nanocomposite is recorded from the DMA when compared to that from the DSC as shown in Table 2, due to the complementary effect of the oscillatory tensile mode on the sample.

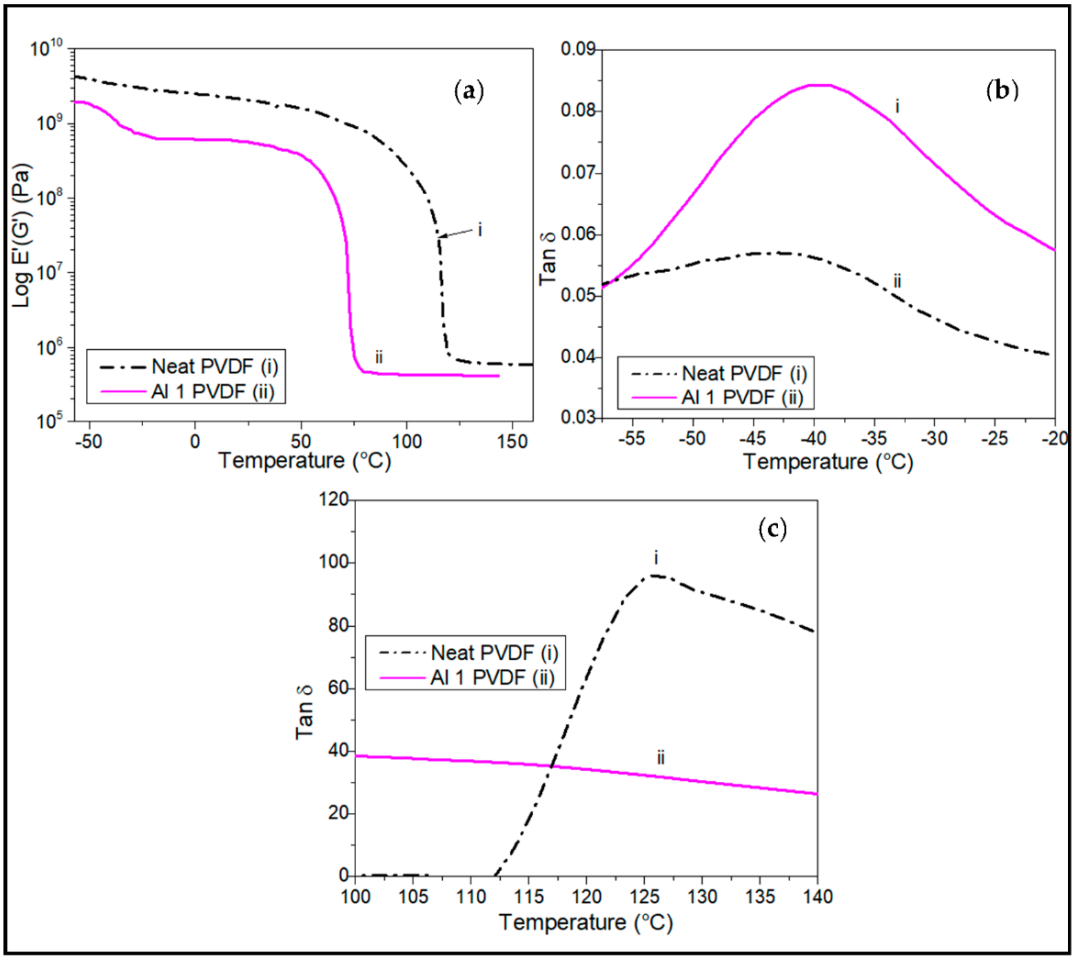

Figure 9. DMA plots comparing the (**a**) **effect of alumina wt.% on** storage modulus of the PVDF nanocomposites at an oscillatory frequency of 1Hz under tension. Tan delta peaks show (**b**) dynamic Tg between −55 °C and −20 °C and (**c**) T_m between 105 °C and 140 °C.

Table 4. Summary of glass transition temperature (T_g) and melting temperature (T_m) measured using DMA at 1 Hz.

Composite	T_g (°C)	T_m (°C)
Neat PVDF	−42.6	125.2
CNT10 PVDF	−44.3	127.0
CNT 50 PVDF	−39.4	-
CNT 1 Al_2O_3 1 PVDF	−42.6	129.2
CNT 10 Al_2O_3 1 PVDF	−37.5	117.7
CNT 1 Al_2O_3 10 PVDF	−33.2	119.9

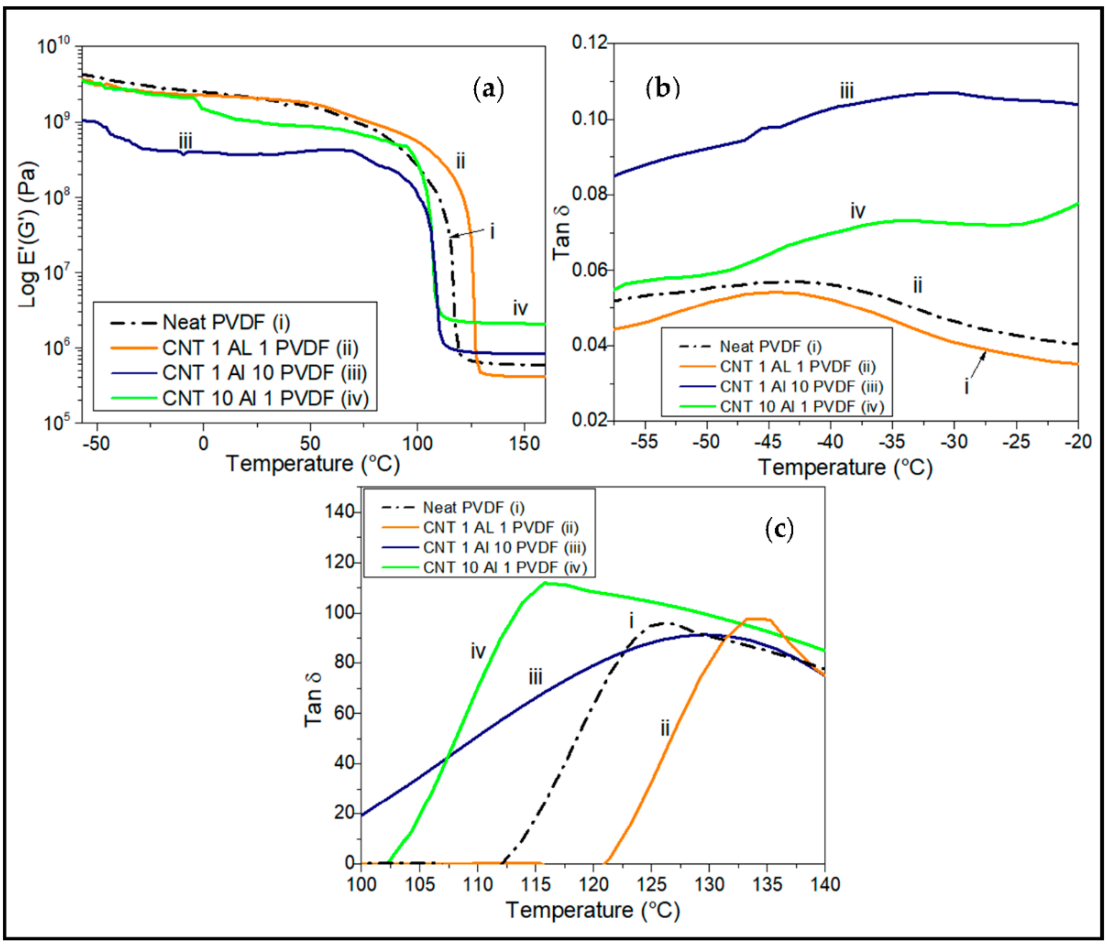

Figure 10. DMA plots comparing the (**a**) **effect of combinatorial wt.% loading of CNT and alumina on the** storage modulus of the PVDF nanocomposites at an oscillatory frequency of 1 Hz under tension. Tan delta peaks show (**b**) dynamic Tg between −55 °C and −20 °C, and (**c**) T_m between 105 °C and 140 °C.

4. Conclusions

In summary, PVDF reinforced with alumina and single-walled carbon nanotube nanocomposites were fabricated by solution blending and cast into thin films. The thermal stability of the nanocomposites was observed to be reduced by the addition of these nanofillers, with alumina showing the most drastic degradation because of preignition reactions that occur with the PVDF melt. Reinforcement with SWCNTs did not make a significant impact on the degradation temperature of the PVDF matrix which remained nearly constant at 420 °C. However, the presence of SWCNT resulted in a higher residual mass of about 63% at 600 °C. Increasing the nanofiller loadings showed a significant increase in the glass transition temperature to as high as −33.2 °C, as well as an increase in the storage modulus to around 18 GPa for composites containing 50 wt.% CNT at −55 °C. The pre-ignition properties of the composite could increase the porosity in the matrix, while the SWCNTs make it electrically conductive. For energy storage applications where porosity and electrical conductivity are important, these two properties make the nanocomposite a very interesting candidate as an electrode material. Furthermore, the composite shows energetic properties that may find potential application in solid-state fuel systems.

Author Contributions: Conceptualization, J.O.I. and R.G.; methodology, J.O.I. and R.G.; software, R.G.; validation, J.O.I. and, R.G.; formal analysis, R.G.; investigation, J.O.I. and. R.G.; resources, J.O.I.; data curation, R.G.; writing—original draft preparation, R.G.; writing—review and editing, J.O.I.; visualization, J.O.I.; supervision, J.O.I.; project administration, J.O.I.; funding acquisition, J.O.I. All authors have read and agreed to the published version of the manuscript.

Funding: This research received no external funding.

Institutional Review Board Statement: Not applicable.

Informed Consent Statement: Not applicable.

Data Availability Statement: Not applicable.

Acknowledgments: The authors acknowledge the assistance provided by the Department of Mechanical and Materials Engineering Department, University of Cincinnati.

Conflicts of Interest: The authors declare no conflict of interest.

References

1. Ma, J.; Haque, R.I.; Larsen, R.M. Crystallization and mechanical properties of functionalized single-walled carbon nanotubes/polyvinylidene fluoride composites. *J. Reinf. Plast. Compos.* **2012**, *31*, 1417–1425. [CrossRef]
2. Kang, G.; Cao, Y. Application and modification of poly(vinylidene fluoride) (PVDF) membranes—A review. *J. Memb. Sci.* **2014**, *463*, 145–165. [CrossRef]
3. Zulfiqar, S.; Zulfiqar, M.; Rizvi, M.; Munirt, A. Study of the thermal degradation of polychlorotrifluoroethylene, poly (vinylidene fluoride) and copolymers of chiorotrifluoroethylene and vinylidene fluoride. *Polym. Degrad. Stab.* **1994**, *43*, 423–430. [CrossRef]
4. Wan, C.; Bowen, C.R. Multiscale-structuring of polyvinylidene fluoride for energy harvesting: The impact of molecular-, micro- and macro-structure. *J. Mater. Chem. A* **2017**, *5*, 3091–3128. [CrossRef]
5. Cao, Y.; Deng, Q.; Liu, Z.; Shen, D.; Wang, T.; Huang, Q.; Du, S.; Jiang, N.; Lin, C.-T.; Yu, J. Enhanced thermal properties of poly (vinylidene fl uoride) composites with ultrathin nanosheets of MXene. *RSC Adv.* **2017**, *7*, 20494–20501. [CrossRef]
6. Kabir, E.; Khatun, M.; Nasrin, L.; Raihan, M.J.; Rahman, M. Pure β-phase formation in polyvinylidene fluoride (PVDF)—Carbon nanotube composites. *J. Phys. D Appl. Phys.* **2017**, *50*, 163002. [CrossRef]
7. Feng, C.-X.; Duan, J.; Yang, J.-H.; Huang, T.; Zhang, N.; Wang, Y.; Zheng, X.-T.; Zhou, Z.-W. Carbon nanotubes accelerated poly (vinylidene fluoride) crystallization from miscible poly (vinylidene fluoride)/poly (methyl methacrylate) blend and the resultant crystalline morphologies. *Eur. Polym. J.* **2015**, *68*, 175–189. [CrossRef]
8. Wang, C.; Qin, M.; Yi, Z.; Deng, H.; Wang, J.; Sun, Y.; Luo, G.; Shen, Q. Oxidation Mechanism of Core-Shell Structured Al @ PVDF Powders Synthesized by Solvent/Non-Solvent Method. *Materials* **2022**, *15*, 3036. [CrossRef]
9. Qamar, Z.; Zakria, M.; Shakoor, R.I.; Raffi, M.; Mehmood, M.; Mahmood, A. Reinforcement of electroactive characteristics in polyvinylidene fluoride electrospun nanofibers by intercalation of multi-walled carbon nanotubes. *J. Polym. Res.* **2017**, *24*, 39. [CrossRef]
10. Remanan, S.; Padmavathy, N.; Rabiya, R.; Ghosh, S.; Das, T.K.; Bose, S.; Sen, R.; Das, N.C. Converting polymer trash into treasure: An approach to prepare MoS2 nanosheets decorated PVDF sponge for oil/water separation and antibacterial applications. *Ind. Eng. Chem. Res.* **2020**, *59*, 20141–20154. [CrossRef]
11. Mokhtari, F.; Spinks, G.M.; Sayyar, S.; Foroughi, J. Dynamic Mechanical and Creep Behaviour of Meltspun PVDF Nanocomposite Fibers. *Nanomaterials* **2021**, *11*, 2153. [CrossRef] [PubMed]
12. Ouyang, Y.; Deng, Y.; Li, D.; Cai, Z.; Xu, R.; Lei, C. Electrical and Thermal Properties of Surface Nanotube/Polyvinylidene Fluoride Composites. *IET Nanodielectr.* **2018**, *1*, 122–126. [CrossRef]
13. Ghosh, S.K.; Das, T.K.; Ganguly, S.; Paul, S.; Nath, K.; Katheria, A.; Ghosh, T.; Chowdhury, S.N.; Das, N.C. Carbon nanotubes and carbon nanofibers based co-continuous thermoplastic elastomeric blend composites for efficient microwave shielding and thermal management. *Compos. Part A Appl. Sci. Manuf.* **2022**, *161*, 107118. [CrossRef]
14. Du, F.-P.; Qiao, X.; Wu, Y.-G.; Fu, P.; Liu, S.-P.; Zhang, Y.-F.; Wang, Q.-Y. Fabrication of porous polyvinylidene fluoride/multi-walled carbon nanotube nanocomposites and their enhanced thermoelectric performance. *Polymers* **2018**, *10*, 797. [CrossRef] [PubMed]
15. Pereira, E.C.L.; Barra, G.M.O.; Soares, B.G.; Silva, A.A. Master batch approach for developing PVDF/EVA/CNT nanocomposites with co-continuous morphology and improved electrical conductivity. *J. Appl. Polym. Sci.* **2021**, *138*, 51164. [CrossRef]
16. Chiu, F.; Chuang, Y.; Liao, S.; Chang, Y. Comparison of PVDF/PVAc/GNP and PVDF/PVAc/CNT ternary nanocomposites: Enhanced thermal/electrical properties and rigidity. *Polym. Test.* **2018**, *65*, 197–205. [CrossRef]
17. Delisio, B.; Hu, X.; Wu, T.; Egan, G.C.; Young, G.; Zachariah, M.R. Probing the Reaction Mechanism of Aluminum/Poly(vinylidene fl uoride) Composites. *J. Phys. Chem. B* **2016**, *120*, 5534–5542. [CrossRef]
18. Knott, M.C.; Craig, A.W.; Shankar, R.; Morgan, S.E.; Iacono, S.T.; Mates, J.E.; McCollum, J.M. Balancing processing ease with combustion performance in aluminum/PVDF energetic filaments. *J. Mater. Res.* **2020**, *36*, 203–210. [CrossRef]

19. McCollum, J.; Morey, A.M.; Iacono, S.T. Morphological and Combustion Study of Interface Effects in Aluminum-Poly(vinylidene fluoride) Composites. *Mater. Des.* **2017**, *134*, 64–70. [CrossRef]
20. Huang, B.C.; Jian, G.; Delisio, J.B.; Wang, H.; Zachariah, M.R.; Wang, H. Electrospray Deposition of Energetic Polymer Nanocomposites with High Mass Particle Loadings: A Prelude to 3D Printing of Rocket Motors. *Adv. Eng. Mater.* **2014**, *17*, 95–101. [CrossRef]
21. Kim, D.W.; Kim, K.T.; Min, T.S.; Kim, K.J.; Kim, S.H. Improved Energetic-Behaviors of Spontaneously Surface-Mediated Al Particles. *Sci. Rep.* **2017**, *7*, 4659. [CrossRef]
22. Pantoya, M.L.; Dean, S.W. Thermochimica Acta The influence of alumina passivation on nano-Al/Teflon reactions. *Thermochim. Acta* **2009**, *493*, 109–110. [CrossRef]
23. Osborne, D.T.; Pantoya, M.L. Effect of Al particle size on the thermal degradation of Al/Teflon mixtures. *Combust. Sci. Technol.* **2007**, *179*, 1467–1480. [CrossRef]
24. Xiao, Y.-J.; Wang, W.-Y.; Chen, X.-J.; Lin, T.; Zhang, Y.-T.; Yang, J.-H.; Wang, Y.; Zhou, Z.-W. Composites: Part A Hybrid network structure and thermal conductive properties in poly (vinylidene fluoride) composites based on carbon nanotubes and graphene nanoplatelets. *Compos. Part A Appl. Sci. Manuf.* **2016**, *90*, 614–625. [CrossRef]
25. Li, Y.; Li, X.; Xiang, F.; Huang, T.; Wang, Y.; Wu, J. properties of PLLA/PEG blend with multiwalled carbon nanotubes. *Polym. Adv. Technol.* **2011**, *22*, 1959–1970. [CrossRef]
26. Cheng, L.; Huang, C.; Yang, Y.; Li, Y.; Meng, Y.; Li, Y.; Chen, H.; Song, D.; Artiaga, R. Preparation and Combustion Performance of B/PVDF/Al Composite Microspheres. *Propellants Explos. Pyrotech.* **2020**, *45*, 657–664. [CrossRef]
27. Chrissafis, K.; Bikiaris, D. Thermochimica Acta Can nanoparticles really enhance thermal stability of polymers? Part I: An overview on thermal decomposition of addition polymers. *Thermochim. Acta* **2011**, *523*, 1–24. [CrossRef]
28. Yang, S.; Rafael, J.; Barrera, E.V.; Lozano, K. Thermal analysis of an acrylonitrile—Butadiene—Styrene/SWNT composite. *Polym. Degrad. Stab.* **2004**, *83*, 383–388. [CrossRef]
29. Liu, Y.; Ma, J.; Liu, W.; Bian, F.; Li, X. Free radical decay and micro-structure evolution of PVDF membranes in situ irradiated by synchrotron radiation X-ray. *Polym. Test.* **2022**, *108*, 107507. [CrossRef]